

Article

Centrifuge Modelling of the Load-Deflection Response of Single Piles in Sand Under One-Way Cyclic Lateral Loads

Bouafia Ali

Department of Civil Engineering, Faculty of Technology, University of Blida1, Blida 09000, Algeria
Correspondance : Bouafia Ali (ali.bouafia@univ-blida.dz)

Abstract: This article aims to present the experimental results of one-way cyclic lateral loading tests on centrifuged small-scale models of piles in sand, carried out in the IFSTTAR centrifuge, center of Nantes (France). After a literature review, the pile models, their instrumentation, the experimental devices, as well as the construction of the sand mass were described. Cyclic P-Y lateral reaction curves were derived and the effect of the number of cycles, the soil density, the pile/soil interface roughness, as well as the pile/soil stiffness ratio on their parameters were analyzed. The experimental evolution of the pile top deflection as well as the bending moment along the pile were compared to the usual formulations of the cyclic degradation law.

Keywords: Centrifuge, Cyclic Loading, Pile, P-Y Curve, Sand.

1. Introduction

Within the framework of geotechnical limit state design (LSD) of usual structures built on pile foundation groups, the lateral response of pile foundations should usually be analyzed by checking the serviceability limit state (SLS). For other structures like the off-shore platforms, wind turbines, high-rise buildings, and port quays, additional checking of the ultimate limit state (ULS) should be performed. SLS design involves the pile displacement analysis, whereas the ULS design involves the determination of lateral pile resistance.

Due to its 3D nature and the multitude of key parameters involved in the lateral pile/soil interaction, this latter is a quite complex geotechnical design task. For more than a century, several research works have been undertaken to explore such a topic, and the literature is quite rich in terms of findings and recommendations. In engineering practice, laterally loaded piles are designed either by measurement from a lateral loading test or predicted based on some commonly used methods, such as Elasticity-based methods [1-4], numerical methods [5], or the P-Y curves methods [6-9].

Theoretical computational approaches are insufficient to provide a realistic description where the lateral pile/soil interaction is modeled using simplistic mechanisms neglecting some key factors, like the technique of pile installation into the soil and the roughness of the pile/soil interface [10].

Nonetheless, within the scope of a pragmatic insight overcoming the inherent uncertainties due to the pile/soil interaction modeling, the pile design is usually undertaken by loading tests leading to a direct measurement of the required design parameters like the pile deflection under working loads and the bending moment along the pile. Due to the relatively

high cost of such a test, this approach is only used to design pile foundations of important projects.

The cyclic lateral loading of deep foundations is frequently encountered in engineering practice, the source of such a loading being either natural (wind, off-shore waves, earthquake, etc.) or industrial (machine vibrations, traffic, etc.). The pile/soil system may be subjected to severe cyclic lateral forces causing a degradation of the lateral soil stiffness and leading to a progressive amplification of the pile deflections. Another effect of cyclic loading is the gradual weakening of the soil resistance and/or the lateral pile resistance after a particular number of cycles. In both cases, the pile/soil system may reach an SLS state by exceedance of the limit displacement prescribed by the structure or a ULS state by exceedance of the lateral resistance.

The cyclic loading may be applied in two senses or one sense, the first one is called a two-way loading, whereas the second one is called a one-way loading. Fig. 1 illustrates a flow chart describing the problem of the pile design under cyclic lateral loading and the methodology of analysis to be adopted. As it may be noticed, a focus was made on the computational design by the P-Y curves method, because it is the most commonly used in practice. This method involves dividing the pile into pieces, defining the P-Y curves at each segment, and then feeding that data into software that calculates a lateral loaded pile.

According to Fig. 1, there are three possibilities for using the P-Y curves method. The first one is a direct use of cyclic P-Y curves, whereas the second one is the use of monotonic P-Y curves to be modified by some "local degradation laws" to account for the effect of the cyclic loading. The last possibility is using the monotonic P-Y curves, the results obtained by computation being modified by some "global degradation

laws", as it will be seen hereafter. It is to be noted that the first possibility is relatively laborious because of the complexity of the construction of the hysteretic loops as recommended in the literature, the second and the third ones are more commonly used.

The experimental findings that follow are a component of a significant research effort that has been conducted for more than 50 years in France by the IFSTTAR (previously LCPC: Laboratories Central des Ponts & Chaussées). A sequence of one-way cyclic lateral stresses was applied to small centrifuged models of single piles, at a scale of 1/18 or 1/20, immersed in a uniform dry sandy mass inside the centrifuge. Having described the complete instrumentation of these models, the paper focuses on fitting, double differentiation, and double integration of the bending moments along the pile to create the experimental P-Y curves. The section concluded by analyzing the effects of the cyclic loading on the P-Y curve parameters, bending moment profiles, and load-deflection curves, specifically the secant lateral response modulus.

2. Centrifuge Modeling in Soil Mechanics

The use of numerical calculations in geotechnical engineering has dramatically increased as a result of the rapid breakthroughs in computer engineering. However, certain numerical models, particularly those in 3D, demand high computational capacities and are therefore time-consuming. Moreover, numerical methods require the input of the soil constitutive law, this latter being currently poorly known.

The full-scale testing is a pragmatic alternative to numerical modeling, but it is limited by the cost and time required, as well as by the quasi-impossibility of carrying out a parametric study. Consequently, this tool is reserved for important research projects.

Experimentation on small-scale physical models may be considered a third way of modeling in soil mechanics and an interesting complement to traditional research tools. However, certain so-called similarity conditions must be respected. These latter are relationships between the different scales derived from the conservation of the governing equations of the phenomenon in the prototype and the model, and are generally obtained by writing the indefinite equations of dynamics, the material constitutive law, and the boundary conditions of the problem.

The components σ_{ij} of the stress tensor acting on a point within a continuum are described by Equation (1):

$$\sum_j \frac{\partial \sigma_{ij}}{\partial x_j} + \rho_i \cdot g_i = \rho_i \frac{\partial^2 u_i}{\partial t^2} \quad i, j = 1, 3 \quad (1)$$

ρ , g , u , x , and t are respectively the components of the unit mass, gravity acceleration, displacement, abscissa, and time along the axis i .

The scale q^* of a physical quantity q is defined as the ratio of this quantity in the model to that in the prototype ($q^* = q_m/q_p$). By writing (1) for the model and the prototype, and introducing the scales q^* , the two following equations may be obtained:

$$\sigma^* = \rho^* g^* L^* \quad (2)$$

$$u^* = g^* (t^*)^2 \quad (3)$$

L^* being the scale of the dimensions. The previous equations, called "the general similitude conditions" are to be absolutely verified. It should be noted that neither hypothesis has been made regarding the constitutive law of the material nor the type of loading.

Due to the inherent nonlinearity of the stress-strain relationship for soils, stresses and strains should be conserved in the model and prototype ($\sigma^*=1$). If we also use the same material ($\rho^*=1$) to preserve its natural properties, Equation (2) implies that:

$$g^* = \frac{1}{L^*} \quad (4)$$

Consequently, a small-scale model is under the same stresses and strains as the prototype if its weight is at a scale inverse to that of the dimensions. Table 1 summarizes the similitude scales of usual physical quantities derived from (4).

Various experimental techniques have been used to apply this theory, among which is the "model centrifugation technique", consisting of combining a centrifuge acceleration with gravitational acceleration, which results in a macro-gravity environment with an acceleration equal to $N_g g$, N_g being the inverse of the scale reduction: $N_g = 1/L^*$ [10]. This technique is the most commonly used, and currently has a considerable worldwide development [11], [12].

As shown in Fig. 2, the IFSTTAR geotechnical centrifuge, center of Nantes, is essentially composed of a pivot carrying a horizontal arm length of 5.5 m, a swinging basket receiving the test container where the physical model is installed. The counterweight behind the arm serves to balance the dynamic unbalance during the rotation of the centrifuge. The highest acceleration of this centrifuge is 200 times that of gravity (g), and the model's maximum mass is 2000 kg at 100g and 500 kg at 200g [13].

Table 1. Summary of usual similitude scales in centrifuge modeling.

Parameter q	Scale q^*
Dimension L	L^*
Gravity acceleration g	$g^*=1/L^*$
Unit mass ρ	$\rho^*=1$
Stress σ	$\sigma^*=1$
Strain ε	$\varepsilon^*=1$
Displacement u	$u^*=L^*$
Force F	$F^*=(L^*)^2$
Moment m	$m^*=(L^*)^3$
Flexural stiffness ($E_p I_p$)	$(E_p I_p)^*=(L^*)^4$
Angle of friction ϕ	$\phi^*=1$

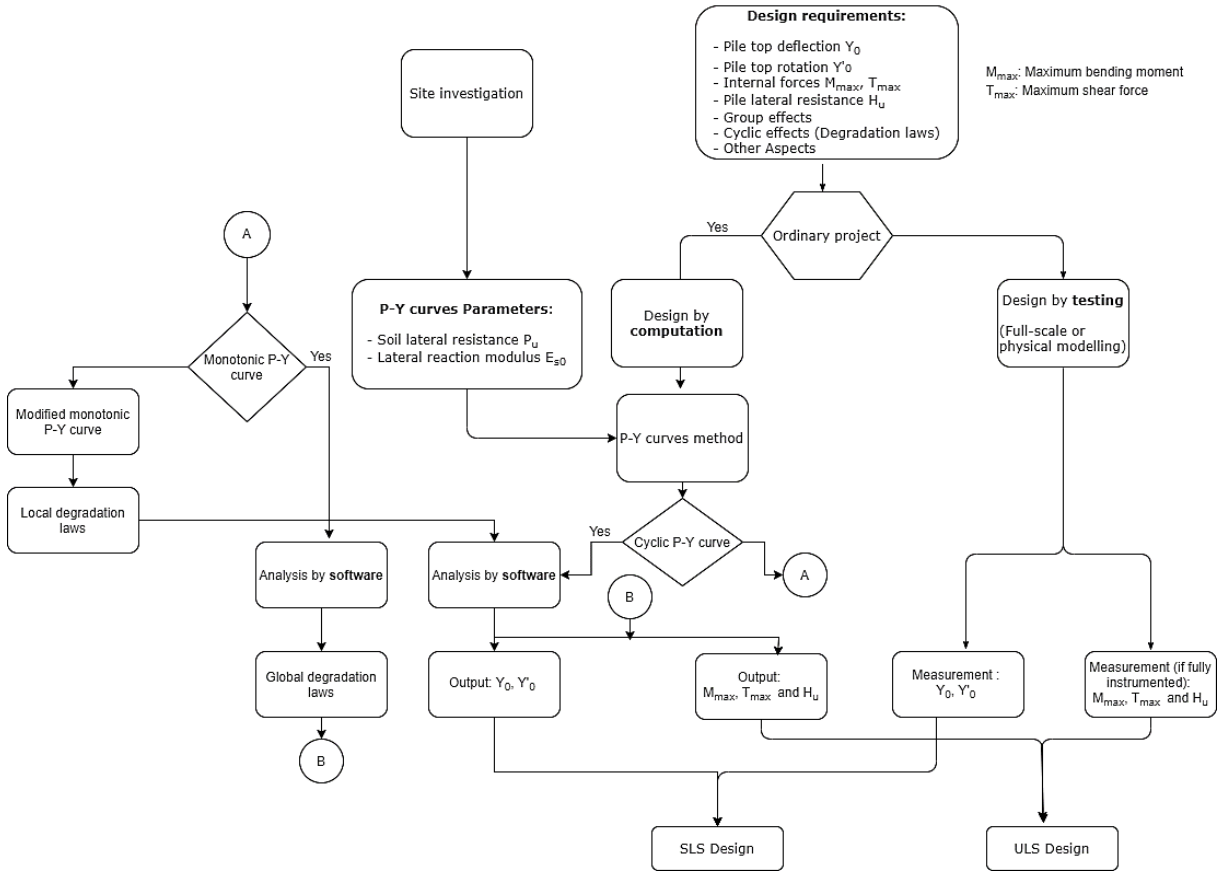


Figure 1. Flow chart of the pile design under cyclic lateral load.

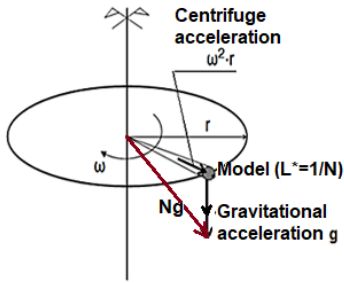


Figure 2. Scheme of centrifuge acceleration (Left) and photo of the IFSTTAR's centrifuge (right).

3. Brief Review of Cyclic Lateral Loading of Pile in Sand

3.1. Degradation Laws for Load-Deflection Curve and P-Y Curves

As illustrated by Fig. 1, the pile top deflection $Y_0(N)$ under a load H , applied at the cycle N , may be derived from the deflection $Y_0(1)$ under the same load H , applied at the first cycle, by using a "global degradation law" $f(N)$, which usually takes the form of a logarithmic function or a power function of the number of cycles N , as follows [14]:

$$\frac{Y_0(N)}{Y_0(1)} = f(N) = 1 + \alpha_y \ln(N) \quad (5)$$

$$\frac{Y_0(N)}{Y_0(1)} = f(N) = N^{\beta_y} \quad (6)$$

Here α_y and β_y , usually called the "degradation parameters", quantify the amplification of the pile deflection due to the cyclic loading; $Y_0(1)$ may be determined by measurement during a monotonic pile loading test, or by computation based on the methods mentioned in the introduction.

Another form of the effect of the cyclic loading on the load-deflection curve is the reduction of the lateral stiffness $K_{AH}(N)$, which is defined as the ratio of the load $H(N)$ to the pile top deflection $Y_0(N)$ at the cycle N . Two possible definitions are usually used. The first one is the "absolute lateral stiffness" $K_{AH}(N)$, which is the slope of the secant line at a load $H(N)$, as depicted in Fig. 3, $H(N)$ being taken for example as the maximal lateral load:

$$K_{AH}(N) = \frac{H(N)}{Y_0(N)} \quad (7)$$

The second definition is the "relative lateral stiffness" $K_{RH}(N)$ which is the ratio of the difference $\Delta H = H_{max} - H_{min}$ to the corresponding difference of pile deflection $\Delta Y_0 = Y_0^{max}(N) - Y_0^{min}(N)$ at the cycle N , as shown in figure 3 [15]:

$$K_{RH}(N) = \frac{H_{max}(N) - H_{min}(N)}{Y_0^{max}(N) - Y_0^{min}(N)} \quad (8)$$

Combining (7) with (5) and (6) leads to writing respectively the degradation laws of the absolute lateral stiffness as follows:

$$\frac{K_H(N)}{K_H(1)} = \frac{1}{f(N)} = \frac{1}{1 + \alpha_y \ln(N)} \quad (9)$$

$$\frac{K_H(N)}{K_H(1)} = \frac{1}{f(N)} = N^{-\beta_y} \quad (10)$$

Similar global degradation laws may be defined for the maximum bending moment, which are expressed by (11) and (12):

$$\frac{M_{max}(N)}{M_{max}(1)} = g(N) = 1 + \alpha_M \ln(N) \quad (11)$$

$$\frac{M_{max}(N)}{M_{max}(1)} = g(N) = N^{\beta_M} \quad (12)$$

α_M and β_M are the degradation parameters corresponding to the maximum bending moment.

The monotonic P-Y curve, at a depth z along the pile, may be modified by a local degradation law to take into account the effect of cyclic loading. The "absolute secant lateral reaction modulus" $E_{AS}(z, N)$ is defined as the ratio $P(z)/Y(z)$ for a given load H at the cycle N :

$$E_{AS}(z, N) = \frac{P(z, N)}{Y(z, N)} \quad (13)$$

As shown in Fig. 4, it is possible to define the "relative secant lateral reaction modulus" $E_{RS}(N)$ as the ratio of the difference $\Delta P = P_{max} - P_{min}$ to the corresponding difference of pile deflection $\Delta Y = Y_{max}(N) - Y_{min}(N)$ at the cycle N :

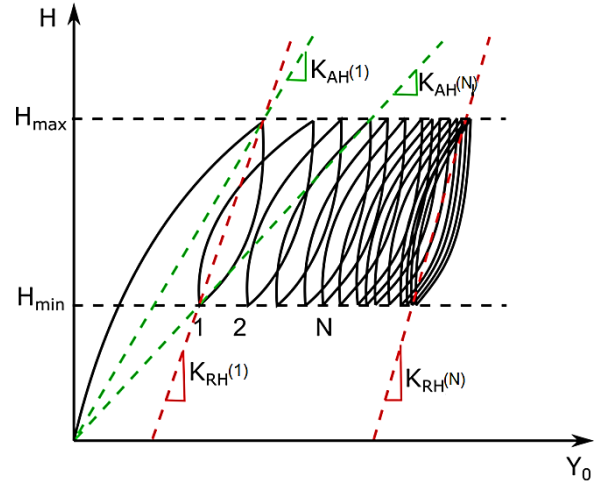


Figure 3. Definition of the cyclic lateral stiffness $K_H(N)$.

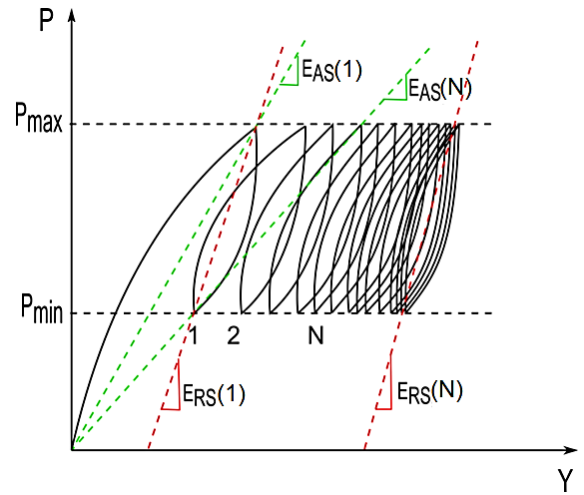


Figure 4. Definition of the secant lateral reaction modulus $E_s(N)$.

$$E_{RS}(z, N) = \frac{P_{max}(z, N) - P_{min}(z, N)}{Y_{max}(z, N) - Y_{min}(z, N)} \quad (14)$$

The absolute modulus E_{AS} is used for the initial state, whereas the relative modulus E_{RS} at cycle N is used concerning the previous cycle. According to the following logarithmic or power degradation laws, the absolute secant lateral reaction modulus $E_{AS}(N)$, corresponding to the cycle N , may be computed as:

$$E_{AS}(N) = E_{AS}(1)[1 + \alpha_E \ln(N)] \quad (15)$$

$$E_{AS}(N) = E_{AS}(1)N^{\beta_E} \quad (16)$$

Here α_E and β_E are the degradation parameters corresponding to the secant lateral reaction modulus at a depth z , for a given lateral load H applied at the pile top. The constants α and β that describe the maximum bending moment, the secant lateral reaction modulus, and the cyclic deterioration of the pile deflection will be the main emphasis of this article.

3.2. Full-Scale Tests ($g^*=1$ and $L^*=1$)

References [16] and [17] carried out full-scale tests on a variety of pile materials (timber, prestressed reinforced concrete, steel), installed into fine or medium-grained sands or silts.

Reference [18] carried out 34 full-scale one-way cyclic lateral tests on piles installed by different techniques, with several cycles varying between 5 and 500.

Reference [19] conducted 20 full-scale cyclic lateral loads in sandy soils with several cycles varying between 4 and 100. He discovered that the density of the sand, the method of installing the pile, the stiffness ratio of the pile to the soil, and the kind of cyclic loading all affect the coefficient α_y .

References [20] and [21] carried out a one-way cyclic lateral load on a steel caisson pile driven into a bi-layered soil, located in Plancoet (France), and composed of a low plastic saturated clay (CL) overlying a thick layer of silty sand (SM). The number of cycles reached 10000.

3.3. Laboratory Model Tests ($g^*=1$ and $L^*<1$)

Tests by [22] on small-scale pile models in the sand showed that α_y is 0.7 beyond 100 cycles.

Reference [23] carried out cyclic lateral tests on small-scale models of Aluminum piles in sand with a frequency of 24 cycles/minute until 1000 cycles. An adaptation phenomena was observed in the fact that the top pile deflection rose as the number of cycles increased and that the load-deflection curve tended to be linear.

Reference [24] carried out cyclic lateral loading tests on small-scale models of flexible piles embedded in dry sand, which led to deriving the value of 0.2 for the coefficient α_y .

Reference [25] was based on a two-way cyclic test on acrylic-resin tubes installed into a very dense dry sandy mass to undertake a qualitative study. The analysis of pile displacement and ground movement was done using X-ray image processing. Cyclic P-Y curves composed of multilinear hysteretic loops were proposed.

A small-scale model of the pile was subjected to one-way cyclic lateral stress up to 10,000 cycles in dry or wet sandy soils according to references [26-27] and [28].

3.4. Centrifuged Model Tests ($g^*>1$ and $L^*<1$)

The impact of cyclic stress on the lateral response of pile foundations was examined using centrifuged size models of piles. Reference [29] carried out two-way cyclic lateral loading on pile models installed into dense saturated fine sand. Observations made from these models were used to develop a finite element calculation method following an elastoplastic constitutive law of the soil.

Reference [30] carried out two-way cyclic loading tests on pile models driven at natural gravity, before centrifugation, into medium-dense saturated fine silty sand, and instrumented

by pairs of strain gauges placed inside the tube and irregularly spaced. The lateral loading consisted of a harmonic excitation with a frequency of 1 to 4 Hz. It was observed that beyond 100 cycles, the behavior of the pile stabilized and exhibited an accommodation.

Cyclic loading tests were carried out by [31] on centrifuged small-scale models of piles in very dense sand ($I_D=95\%$) simulating a prototype pile having an embedded length D of 12 m and a diameter B of 0.72 m (slenderness ratio $D/B=16.7$) under a one-way cyclic lateral loading up to 500 cycles.

Reference [32] carried out a series of one-way cyclic lateral loads up to 50 cycles on a centrifuged small-scale model ($g^*=40$) of a flexible pile ($D/B=16.7$) driven into very dense dry sand ($I_D=86-100\%$), the pile/soil interface is smooth.

These tests on the same pile model ($g^*=40$) were subsequently extended by [33] up to 70000 cycles into medium to very dense sand ($I_D=48-78\%$).

Centrifuged small-scale models of piles were used by [34] to carry out one-way cyclic loading up to 100-1000 cycles into very dense dry sand ($I_D=97\%$). It was shown the amplification of the pile top deflections due to cyclic loading may be well described by a logarithmic law.

Table 2 summarizes the values of cyclic degradation coefficients α_y and β_y , in which can be seen discrepancies which may be probably due to the multitude of key factors governing the effect of cyclic lateral response of the piles in the sand such as the sand density, the pile/soil stiffness ratio, the type of cyclic loading, the soil moisture content, and the mode of pile installation. Experimental investigation is therefore needed to explore the cyclic lateral pile/soil response, and the results presented in this paper fall within such a framework.

Fewer studies were published regarding the effect of cyclic loading on the bending moment as well as on the P-Y curves. A possible explanation is that detailed instrumentation of the test pile (by strain gauges, inclinometer, or extensometer) is required to measure the bending moments along the pile, which is relatively expensive and laborious. Nevertheless, using full-scale tests at the site Plancoet, Reference [21] showed that M_{max} increases according to a logarithmic law described by (11). Moreover, the small-scale model tests carried out by [31] showed that α_M for a one-way cyclic loading was found within the margin 0.02-0.05. However, Reference [33] showed that M_{max} increases by 10% at 100 cycles but stabilizes beyond.

Reference [32] showed that the cyclic degradation of M_{max} is well described by a logarithmic function, with a coefficient α_M less than 0.025 and depending on the ratio H_{min}/H_{max} , H_{min} , and H_{max} being respectively the minimum and maximum lateral load applied at the pile top as depicted in Fig. 3.

Table 2. Values of the cyclic degradation coefficients α_v and β_v in sand.

Test	Author	α_v		β_v		
		Margins	Particular values	Margins	Particular values	
Full-scale	Alizadeh & Davisson (1970) [17]	0.7-0.9		0.07-	0.08 in dense sand	
	Long & Vanneste (1994) [18]					0.14
	Lin & Liao (1999) [19]	0.02-0.24		0.18 for flexible driven piles in medium dense sand		
				0.16 for flexible driven piles in dense sand		
	Hadjadi et al (2002) [21]		0.087 at $N=10^4$			
Laboratory model test	Davisson & Salley (1970) [22]		0.7 for $N > 100$			
	Hettler (1981) [24]		0.20			
	Leblanc et al (2010) [26], [27]			0.3		
	Peralta (2010) [28]	0.21		0.12		
Centrifuged model test	Verdure (2003) [31]	0.04-0.18	0.18 under a one-way with $H_{min}=0$			
	Rosquoet (2004) [32]		0.10 under a one-way with $H_{min}=0$			
	Rakotonindriana (2009) [33]		0.15 under a one-way with $H_{min}=0$			
	Li et al (2010) [34]	0.17-0.25				

4. Description of Pile Models and Experimental Devices

4.1. Pile Models

The pile models consist of two Duralumin AU-4G pipes. Laboratory dimensional control made it possible to measure the exact values of the inside and outside diameters. The geometric and mechanical properties of the pile models as well as their prototypes are summarized in Table 3.

As seen in Fig. 5, each pile model is instrumented with 12 pairs of strain gauges adhered to the pipe's outside on two opposing axes. The gauges are covered with a rough adherent layer 1 to 2 mm thick, to protect them against humidity and sand friction [10].

Each model was calibrated based on the scheme of the cantilever beam, to check out the pile flexural stiffness, as well as the normal performance of the strain gauges, by comparing the measured and theoretical strains. An excellent agreement was found with a difference within 4%.

4.2. Loading Device

The lateral force was applied by using the foundation loading device, where a flexible metal cable passing through a pulley is put in tension by the movement of a swinging mass on a loading beam as shown in Fig. 6, the latter could swing around a horizontal axis [10].

4.3. Sand

The sand material, extracted from experimental site Le-Rheu, located at Rennes, France, is classified as a poorly graded sand (SP), and characterized by a mean diameter D_{50} of 0.3 mm, and minimum and maximum dry unit weights of 13.4 kN/m³ and 16.8 kN/m³ respectively. The direct shear tests on dry sand gave a friction angle of 36.3° for loose sand ($I_D=20\%$) and 41.5° for very dense sand ($I_D=85\%$).

The construction of the sand mass at a given density is done by raining the sand in the air around the pile model, using a mobile hopper with adjustable sweeping speed and height of fall. This procedure may be considered as a simulation of the technique of installation of the pile by boring.

4.4. Loading Program

Each pile model was subjected to a one-way cyclic lateral loading up to 2 to 4 cycles (with $H_{min}=0$). The loading program consisted of increments of 50 kN up to 200 kN and 60 kN up to 480 kN in prototype for piles P_1 and P_2 respectively, the duration of each increment in the first cycle was 3 min. For the subsequent cycles, the duration varied with the cycles, from 1 to 3 min for P_1 , and from 1 to 5 min for P_2 . Each test's primary parameters are compiled in Table 4. The results that follow are all of the prototype piles P_1 and P_2 , which were obtained by extrapolating all of the experimental results of the pile model to the prototype scale using the similitude scales of Table 1.

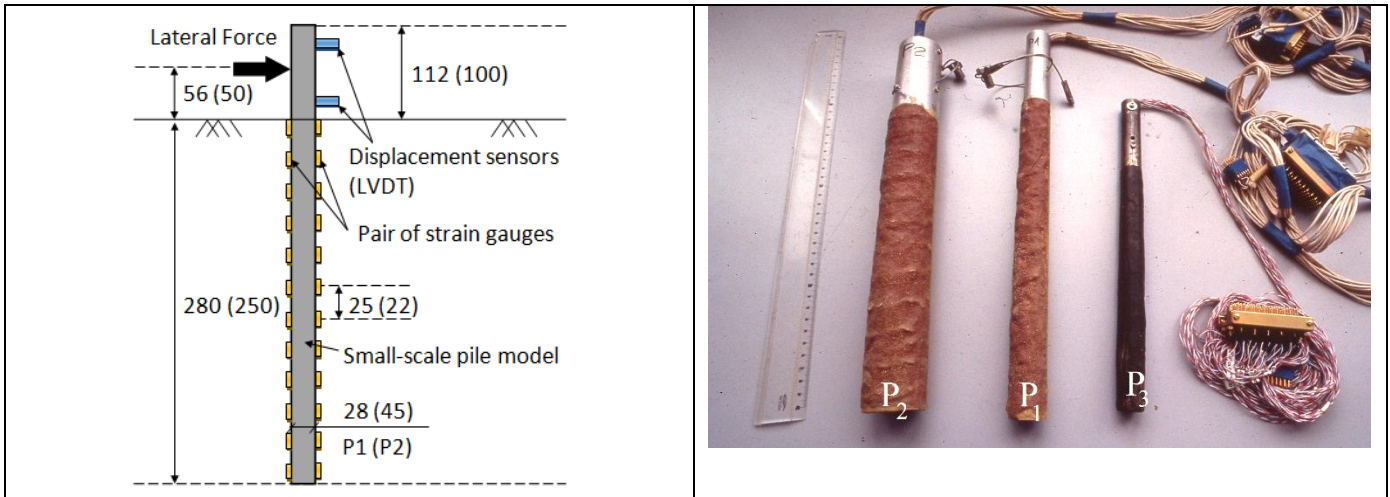


Figure 5. Scheme and photo of instrumentation of a pile model (Dimensions between brackets are for P₂).

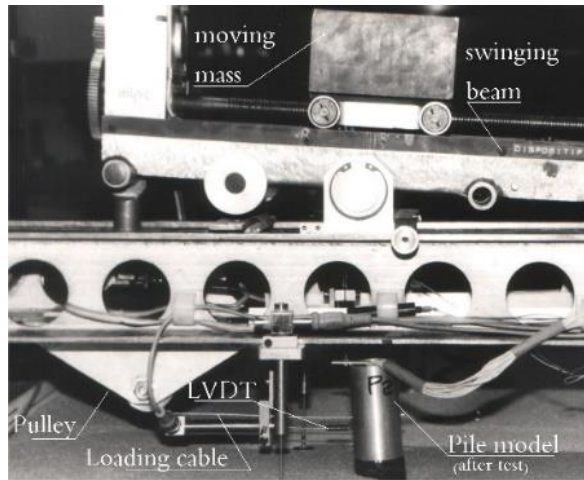


Figure 6. System of lateral loading in the centrifuge (Bouafia, 1990).

Table 3. Properties of the prototype piles and the physical models.

	Pile P ₁		Pile P ₂		Ratio P ₂ /P ₁
	Prototype	Model	Prototype	Model	
Scale L*	1	1/17.85	1	1/20	
Outside diameter B (mm)	500	28.07	900	45.02	1.80
Inside diameter (mm)	456.60	25.58	810.4	40.52	1.77
Embedded length D (mm)	5.0	0.280	5.0	0.250	1.0
Slenderness ratio D/B	10	10	5.5	5.5	0.55
Eccentricity of load e (mm)	56	1000	50	1000	1
Flexural stiffness E _p I _p (Nm ²)	56.65x10 ⁶	558	741 x10 ⁶	4631	13.1
Limit elastic stress σ _e (MPa)	171	171	260	260	1.52
Limit elastic moment M _e (kN.m)	646.8	0.151	6413	801	10.0
Tensile resistance (MPa)	354	354	406	406	1.15

Table 4. Parameters of cyclic lateral tests in the centrifuge.

Pile	Test	Number of cycles	Dry unit weight γ _d (kN/m ³)	Density index I _p (%)	Surface roughness
P ₁	2	4	15.4	63	Smooth
	3	2	16.5	93	Smooth
	15	4	16.6	95	Rough
P ₂	1	2	15.1	57	Smooth
	4	2	16.6	95	Smooth
	15	4	16.6	95	Rough

5. Presentation and Discussion of Results

5.1. Load-Deflection Curves

Fig. 7 illustrates all the load-deflection curves of the piles P_1 and P_2 which are characterized by an inherent nonlinearity of the monotonic portion, even within the domain of small deflections. As can be seen from this figure, by increasing the sand density, the top deflection Y_H of a smooth interface under a maximum lateral load H_{max} decreases by 38.5% for pile P_1 and 73.5% for pile P_2 . A possible explanation is that an increase in density leads the sand to exhibit a contraction behavior, which increases the soil stiffness and therefore reduces the pile displacement.

In line with the findings of centrifuge experiments conducted at the University of Liverpool [35], Y_H under H_{max} drops by 33% for pile P_1 and 20% for P_2 when the roughness of the pile/soil contact within very dense sand is increased. A greater mobilization of the shear strength at a rough pile/soil interface could account for the decrease in pile displacement.

From a smooth pile within medium-dense sand to a rough pile within very dense sand, the cumulative reducing effects of the sand density and the interface roughness led to a decrease of 59.0% for Pile P_1 and 78% for pile P_2 . Such a statement shows that pile P_2 , which is shorter and stiffer than P_1 according to Table 2, exhibits more sensitivity to these two factors. Moreover, the load-deflection curves show a slight increase in pile deflections with the number of cycles. However, beyond the first cycle, the top deflection Y_H for a given lateral load H tends to stabilize.

As shown in Fig. 8, the degradation parameter α_y was determined by fitting the experimental values of $Y_H(N)/Y_H(1)$ as a logarithmic function of N (cycle number), according to (5). As can be seen in this figure, α_y for pile P_1 under $H_{max}=200$ kN decreases from 0.117 for a smooth interface in medium-dense sand to 0.075 for a rough interface in very-dense sand. For pile P_2 under $H_{max}=480$ kN, α_y was found equal to 0.063 for a rough interface in a very dense sand, which is in reasonable accordance with that of pile P_1 having a rough interface and installed into a very dense sand, the slight difference between them is likely due to difference of slenderness ratio and the flexural pile stiffness, as summarized in Table 3. As stated above regarding the effects of the sand density and the interface roughness on the monotonic displacements, it seems that these factors play the same effect on α_y .

By comparing the values of α_y to those summarized in Table 2, it can be noticed that α_y for pile P_1 , considered a relatively flexible pile, with a smooth interface in medium-dense sand, is in good accordance with the results of [32] and [33], and falls within the margin proposed by [19] and [31].

As summarized in Fig. 9, the value of degradation parameter β_y for pile P_1 under $H_{max}=200$ kN is equal to 0.109 for a smooth interface in medium-dense sand, whereas it decreases to 0.071

for a rough interface in very dense sand. Moreover, β_y for pile P_2 under $H_{max}=480$ kN is equal to 0.06 for a rough interface in very dense sand, in good agreement with that of pile P_1 . It is remarkable that the values of β_y are practically equal to α_y , and also exhibit the same variation as α_y as a function of the pile/soil interface roughness and the sand density.

The secant lateral pile stiffness K_{AH} , as formulated by (7), is illustrated in Fig. 10, which shows a slight degradation, as the ratio $K_{AH}(N)/K_{AH}(1)$ decreases with the number of cycles, reaching 0.85 and 0.92 in medium dense and very dense sand respectively. The small difference between the values of piles P_1 and P_2 in test 15 (very dense sand and rough interface) implies that the differences in the pile characteristics have practically a negligible effect. Moreover, the ratio $K_{AH}(N)/K_{AH}(1)$ was predicted by using (9) and the values of the degradation coefficient α_y , which led to a good accordance with that derived from the load-deflection curve.

The relative secant lateral stiffness K_{RH} , determined according to (8), was also found slightly decreasing with the number of cycles in all the tests. Such a statement is confirmed by the loops, describing the one-cyclic response of the test piles, which are practically superimposable, as illustrated in Fig. 7. It is therefore possible to conclude that they may be approximately characterized by a unique relative lateral stiffness K_{RH} .

5.2. Bending Moment Profiles

Fig. 11 illustrates typical profiles of the bending moment along the test pile P_1 under H_{max} , where it can be noticed a very slight decrease, at a given depth, with the number of cycles. In fact, after four cycles, the maximum moment decreases only by 4%.

The values of the cyclic degradation coefficients α_M and β_M , as formulated respectively in (11) and (12), were found practically equal to 0, whatever the sand density, the interface roughness, and the pile characteristics. This fact is by [32] who found α_M less than 0.025.

Additionally, centrifuge testing in the University of Cambridge's sand proved that the depth of the maximum bending moment was unaffected by cyclic loading [29]. It can be seen in Fig. 11 the existence of residual bending moments after the total unloading of the pile, which may be explained by the collapse of the sand on the surface behind the pile, and near the front tip, which prevents the pile from returning to its initial position.

6. Analysis of the P-Y Curves

6.1. Methodology of Construction of P-Y Curves

With P representing the lateral soil response and Y the corresponding pile lateral displacement (or deflection), the P-Y curve is an experimental constitutive law of the pile/soil interface at a given depth.

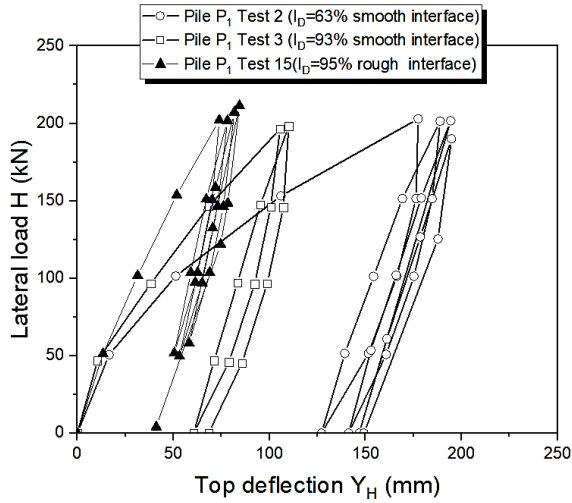


Figure 7. Load-deflection curves of piles P1 and P2.

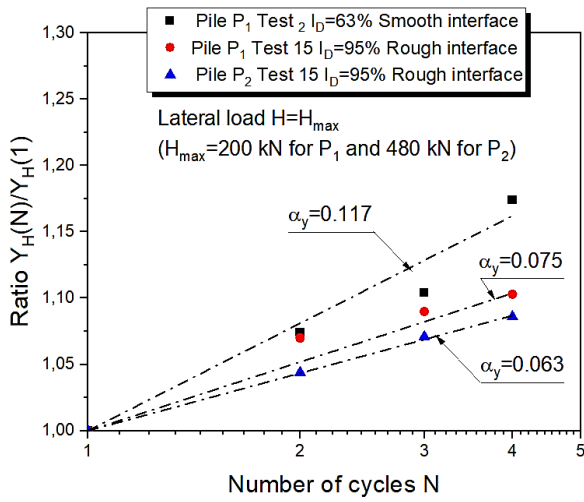
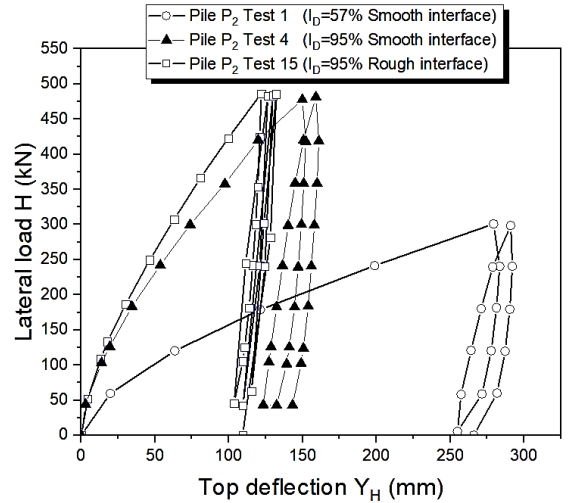


Figure 8. Determination of the degradation parameter α_y .

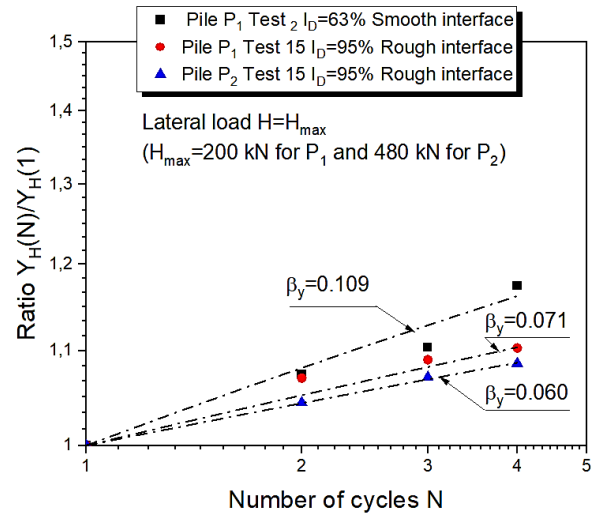


Figure 9. Determination of the degradation parameter β_y .

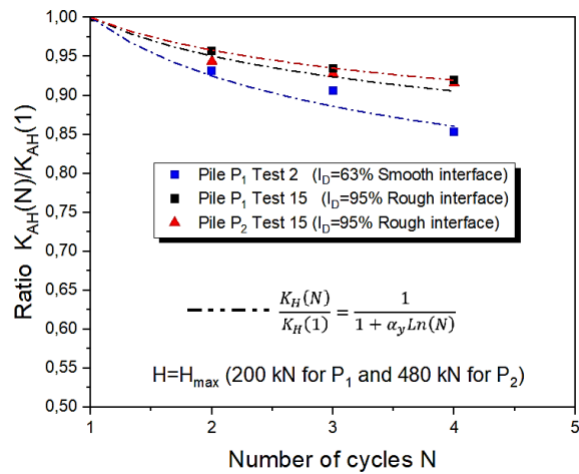


Figure 10. Cyclic degradation of the secant lateral pile stiffness K_{AH} under H_{max} .

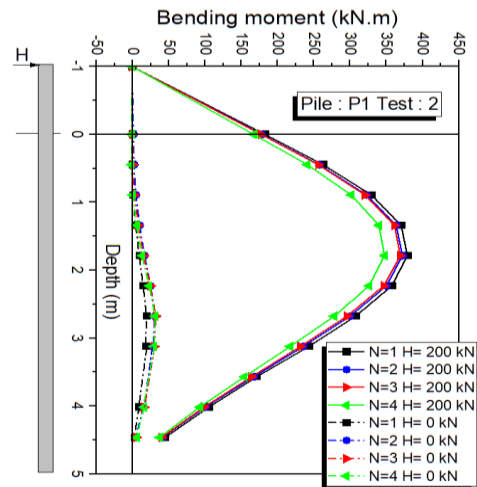


Figure 11. Typical profiles of cyclic bending moment along the pile P1.

The bending moment profile $M(z)$ was fitted and then subjected to a process of successive integrations and differentiations. SLIVALIC 5 software was used to smooth the experimental bending moment profile, under a given lateral load H , by a set of spline functions parameterized by a smoothing coefficient [36]. Two successive integrations allow the determination of the profile of deflections $Y(z)$, taking into account the boundary conditions in terms of displacement Y_0 and rotation Y_0' at the ground surface, as described in (17):

$$Y(z) = \frac{1}{E_p I_p} \int \left(\int M(z) dz \right) dz + Y_0' z + Y_0 \quad (17)$$

The integration constants Y_0 and Y_0' are calculated from the head displacement and rotation measurements. Moreover, two successive differentiations of $M(z)$ lead to determining the soil reaction $P(z)$ and then building the P-Y curves along the pile:

$$P(z) = - \frac{d^2 M(z)}{dz^2} \quad (18)$$

The soil reaction $P(z)$ is highly sensitive to changes in the bending moment values and is thus greatly dependent on the fitting curve of the bending moment profile. This is because $P(z)$ is the curvature of the bending moment profile $M(z)$ at a given depth z [37]. The test pile's static equilibrium under the lateral reaction profile $P(z)$ and the loads on the pile top were used to determine the smoothing parameter, which was then set within a specified tolerance [38].

6.2. P-Y Curves for Monotonic Loading

A typical set of monotonic P-Y curves, corresponding to the first cycle, are illustrated in Fig. 12 for pile P_1 in test 2, where the depth z along the pile is normalized by the pile diameter B . At a normalized depth equal to 7, it can be noticed a simultaneous change in the sign of the deflection Y and the lateral reaction P . This fact is to the fundamental assumption of Winkler, according to which P and Y are proportional and have the same sign [39-40]:

$$P(z) = E_{s0}(z) \cdot Y(z) \quad (19)$$

However, to describe the P-Y function, the non-linear shape of the P-Y curves leads to defining a secant lateral reaction modulus, as formulated in (13), instead of the "initial reaction modulus" E_{s0} appearing in (19). It was found all the experimental P-Y curves may be fitted by the following hyperbolic function:

$$P(z) = \frac{Y(z)}{\frac{1}{E_{s0}(z)} + \frac{Y(z)}{P_u(z)}} \quad (20)$$

E_{s0} is the lateral reaction modulus corresponding to the very small deflection Y of the pile, and P_u is designated as the "lateral soil resistance".

Hyperbolic fitting of the experimental P-Y curves by (20), based on the least square technique, led to deriving the profile of E_{s0} , which is illustrated in Fig. 13. Moreover, the secant modulus E_s for a given lateral load is also shown in this figure, where it can be seen that E_s at a given depth z decreases with the lateral load because of the non-linearity of the P-Y curve. Nonetheless, as expected, all the profiles of the lateral reaction modulus exhibit a linear increase with depth, which is typical in a homogeneous sandy mass, belonging to Gibson's soil category.

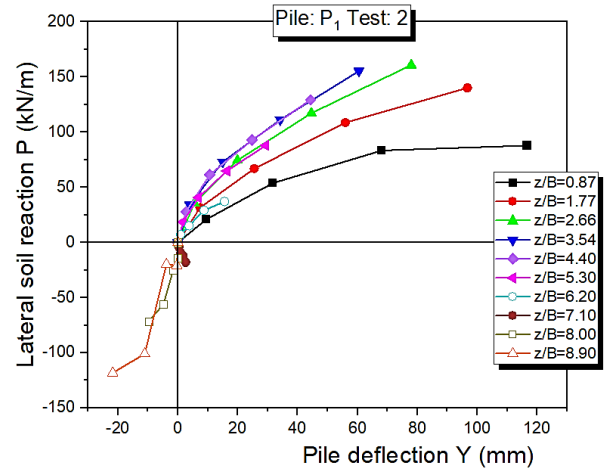


Figure 12. A typical set of monotonic P-Y curves.

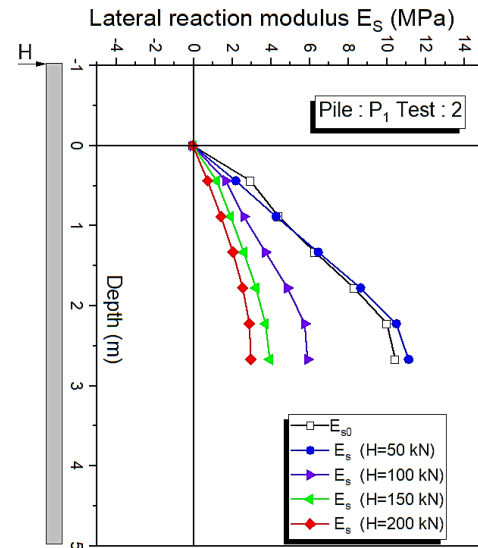


Figure 13. Profiles of the lateral reaction moduli for pile P1 in test 2.

6.3. P-Y Curves for a One-Way Cyclic Loading

According to Fig. 14, the pile deflections of pile P_1 in test 2 under $H_{max}=200$ kN exhibit, at a given depth, a small increase with the number of cycles, particularly in the upper half part of the pile.

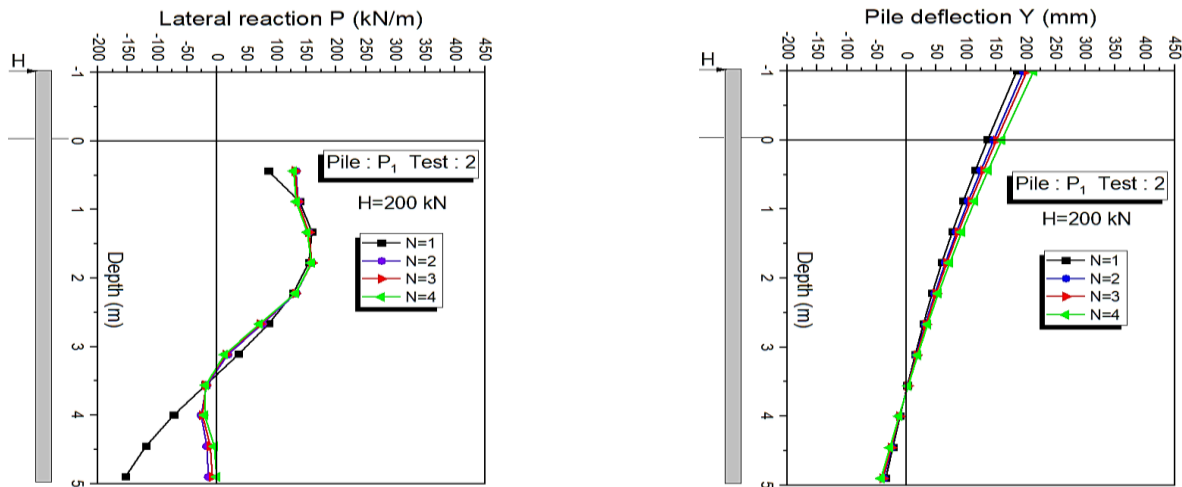


Figure 14. Profiles of pile deflection $Y(z)$ and soil reaction $P(z)$ under cyclic loading H_{max} .

Moreover, for the monotonic lateral reaction, the cyclic $P(z)$ exhibits an increase at a depth of $1B$, beyond which no variation is noticed till a depth of 7 , corresponding to the "rotation center" where P and Y are simultaneously equal to 0 as shown in Fig. 12. Beyond the rotation center, the cyclic $P(z)$ slightly decreases with the number of cycles.

In Fig. 15 are illustrated the cyclic P - Y curves, where it can be noticed the loops may be roughly approximated as a set of average lines that are practically parallel.

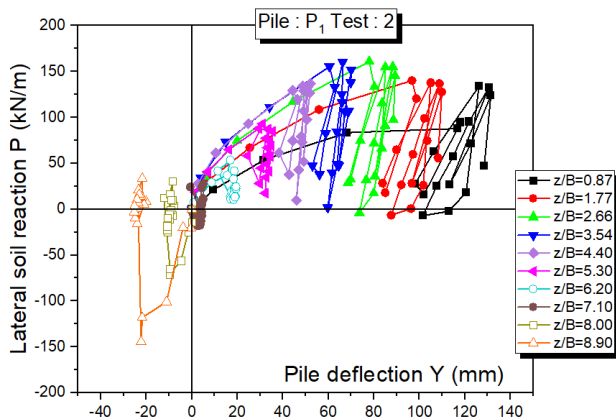


Figure 15. Typical set of one-way cyclic P - Y curves.

6.4. Cyclic Lateral Reaction Modulus

Under a maximum lateral load on pile P_1 in test 2, the absolute secant lateral reaction modulus E_{AS} was computed according to (13) as a function of the number of cycles and its profile illustrated in Fig. 16. As can be seen in this figure, E_{AS} slightly decreases within the upper half part of the pile and considerably decreases beyond the center of rotation.

Fig. 17 shows the profiles of the cyclic degradation coefficients α_E and β_E , as defined in (15) and (16) respectively, where it can be noticed an irregular decrease along the pile, from 0.3 at $1B$ of depth to -0.9 at a depth of $6B$. In light of this

experimental result, it seems the effect of depth on the lateral reaction modulus is not negligible.

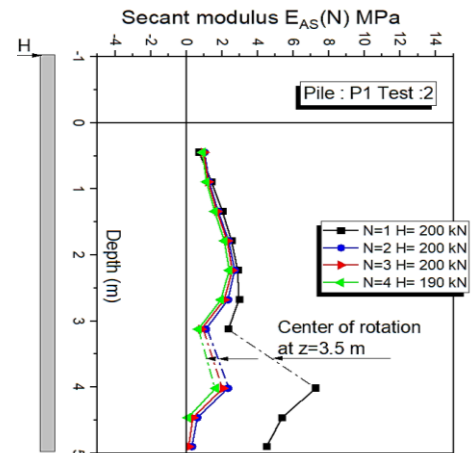


Figure 16. Profiles of the absolute reaction modulus E_{AS} .

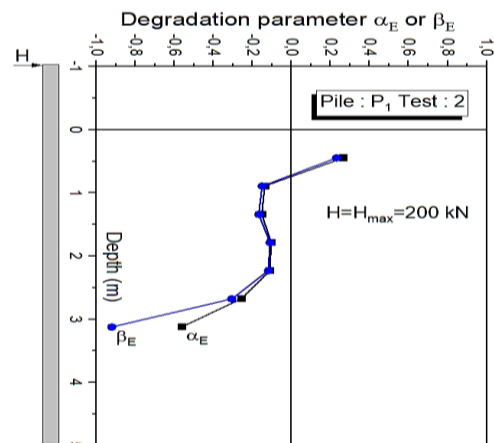


Figure 17. Profiles of the coefficients α_E and β_E .

7. Conclusions

In this paper, the technique of physical modeling in a centrifuge was used to explore the one-way cyclic response of two single piles embedded into a homogeneous deposit of sand. One of the test piles is flexible whereas the other one is rather short and rigid. After a brief review of the similitude theory in soil mechanics as well as the degradation laws for the load-deflection curve and the P-Y curves, the small-scale models of the test piles as well as the experimental devices were described.

The examination of the load-deflection curves revealed that, for a given lateral load at the pile top, pile deflections increased somewhat with the number of cycles and tended to stabilize after the first cycle. Under a maximum lateral load, α_y for the flexible pile P_1 decreases from 0.117 for a smooth interface in medium-dense sand to 0.075 for a rough interface in very dense sand. Good accordance was found with the results obtained from centrifuge tests carried out elsewhere.

For the rigid pile, α_y was found equal to 0.063 for a rough interface in a very dense sand, which is in reasonable accordance with that of the flexible pile having a rough interface and installed into a very dense sand, the slight difference between them is likely due to difference of slenderness ratio and the flexural pile stiffness.

It was remarkably found that β_y exhibits the same variation as α_y as a function of the pile/soil interface roughness and the sand density. The absolute secant lateral pile stiffness K_{AH} decreases with the number of cycles, the ratio $K_{AH}(N)/K_{AH}(1)$ reaching, after 4 cycles, 0.85 and 0.92 in medium-dense and very dense sand respectively. Similarly, the relative secant lateral stiffness K_{RH} was also found slightly decreasing with the number of cycles in all the tests.

The maximum bending moment was found to decrease very slightly, at a given depth, with the number of cycles, up to 4% after 4 cycles. Consequently, the values of the cyclic degradation coefficients α_M and β_M were found practically equal to 0, whatever the sand density, the interface roughness, and the pile characteristics, which is in accordance with the literature.

After outlining the methodology of construction of the P-Y curves, these latter under monotonic as well as one-way cyclic conditions were presented and analyzed. The profiles of initial and secant lateral reaction moduli were remarkably characterized by a linear increase in depth, in accordance with the scheme of Gibson's soils. It was discovered that the absolute secant lateral response modulus (EAs) decreased significantly outside the center of rotation and only somewhat as a function of the number of cycles in the upper half of the pile. The experimental findings highlighted in this paper need to be generalized by extending the number of cycles and studying other pile/soil configurations.

Acknowledgments: The author is grateful to the team of the section MEC (Centrifuge Modeling Section) of the IFSTTAR, center of Nantes, France, for their help in preparing and carrying out the cyclic tests on centrifuged pile models.

Statements and Declarations: The author declares that there are non-financial interests that are directly or indirectly related to the work submitted in this paper. Moreover, it is declared there are no conflicts of interest.

References

- [1] P. K. Banerjee and T. G. Davies, "The behaviour of axially and laterally loaded single piles embedded in nonhomogeneous soils," *Geotechnique*, vol. 28, no. 3, pp. 309–326, 1978., doi: 10.1680/geot.1978.28.3.309
- [2] M. Budhu and T. G. Davies, "Nonlinear analysis of laterality loaded piles in cohesionless soils," *Can. Geotech. J.*, vol. 24, no. 2, pp. 289–296, 1987., doi:DOI: 10.1139/t87-034
- [3] M. F. Randolph, "The response of flexible piles to lateral loading," *Geotechnique*, vol. 31, no. 2, pp. 247–259, 1981., doi: 10.1680/geot.1981.31.2.247
- [4] H. Poulos and T. Hull, *Analytical geomechanics in foundation engineering - A study of laterally loaded piles*, Research report No. R667 to the University of Sydney, Australia, (1992), 40 p.
- [5] H. Haouari and A. Bouafia, "Centrifuge Modelling and Finite Element Analysis of Laterally Loaded single piles in Sand with Focus on P-Y Curves," *Period. Polytech. Civ. Eng.*, vol. 3, 2020., doi: 10.3311/PPci.14472
- [6] H. Matlock and L. C. Reese, "Generalized solutions for laterally loaded piles," *J. Soil Mech. Found. Div.*, vol. 86, no. 5, pp. 63–92, 1960., doi: 10.1061/jsfeaq.0000303 DOI: 10.1061/JSFEAQ.0000303
- [7] L. Ménard, M. Gambin, and G. Bourdon, "Méthode générale de calcul d'un rideau ou d'un pieu sollicité horizontalement en fonction des résultats pressiométriques," *Journal Sols/Soils*, vol. 1, no. 20/23, pp. 16–28, 1969.
- [8] F. Baguelin, J.-F. Jézéquel, and D.-H. Shields, N° 4, vol. 2, 1st ed. Germany: Trans Tech Publications, 1978, The pressuremeter and foundation Engineering, Series on rock and soil mechanics.
- [9] L. Reese and W. Van Impe, *Single piles and pile groups under lateral loading*, edited by Francis and Taylor/Balkema, 2001.
- [10] A. Bouafia, *Modélisation des pieux en centrifugeuse (in French)*, Ph.D Thesis of civil engineering, University of Nantes, 1990, 267 pages.
- [11] J. Garnier, 'The LCPC centrifuge: Tools of preparing models and instrumentation', *Proceedings of Centrifuge 88 International Congress*, Paris, April 25 to 27, (1988), Editor; J.-F. Corté, Balkema, Rotterdam. pp. 83-93.
- [12] J. Garnier, 'The LCPC centrifuge: a new means of testing in microgravity'. *ASTELAB 90 International Conference*, Paris June 11 to 15, 1990. pp. 417-422.
- [13] J.-F. Corté and J. Garnier, "A centrifuge for geotechnical research," *Bulletin of the LCPC Laboratories*, no. 146, 1986.
- [14] A. Puech and J. Garnier, *Design of Piles Under Cyclic Loading-SOLCYP Recommendations*, 1st edition, ISTE Editions, ISBN: 978.178.6301987, (2017), 454 pages.
- [15] H. Haouari and A. Bouafia, "Single piles under monotonic lateral loads-Full scale tests and numerical modelling," *Journal of Geomechanics and Geoengineering*, vol. 1, pp. 11–25, 2022., doi: 10.38208/jgg.v1i1.441
- [16] M. Alizadeh, 'Lateral load tests on instrumented timber piles', *American Society for Testing and Materials 7th Annual Meeting*, San Francisco, June 23-28, 1968, Special Technical Publication 444, pp. 379-394.
- [17] M. Alizadeh and M. T. Davison, "Lateral load tests on piles-arkansas river project," *J. Soil Mech. Found. Div.*, vol. 96, no. 5, pp. 1583–1604, 1970., doi: 10.1061/jsfeaq.0001456 DOI: 10.1061/JSFEAQ.0001456
- [18] J. H. Long and G. Vanneste, "Effects of cyclic lateral loads on piles in sand," *J. Geotech. Eng.*, vol. 120, no. 1, pp. 225–244, 1994.
- [19] S.-S. Lin and J.-C. Liao, "Permanent strains of piles in sand due to cyclic lateral loads," *J. Geotech. Geoenviron. Eng.*, vol. 125, no. 9, pp. 798–802, 1999., doi:DOI: 10.1061/(asce)1090-0241(1999)125:9(798) DOI: 10.1061/(ASCE)1090-0241(1999)125:9(798)
- [20] T. Hadjadji, *Analyse du comportement expérimental de pieux sous chargements horizontaux (In French)*. Ph.D Thesis, Ecole Nationale des Ponts et Chaussées, France, 1993.
- [21] Hadjadji, T., Frank R., Degny, E. *Analyse du comportement expérimental de pieux sous chargements horizontaux (in French)*, LCPC, Collection Etudes et Recherches, GT-74.

- [22] M. T. Davisson and J. R. Salley, "Model study of laterally loaded piles," *J. Soil Mech. Found. Div.*, vol. 96, no. 5, pp. 1605–1627, 1970., doi:DOI: 10.1061/jsfeaq.0001457 DOI: 10.1061/JSFEAQ.0001457
- [23] S. Prakash and V. Chandrasekara, 'Deflections of battered pile groups under cyclic lateral loads', Proceedings of the 2nd Southeast Asian Regional Conference on soil mechanics, June 11-15, Singapore.
- [24] A. Hettler, Verschiebungen starrer und elastischer Gründungskörper in Sand bei monotoner und zyklischer Belastung (in German), Doctoral Thesis, Veröffentlichungen des Instituts für Boden-mechanik und Felsmechanik der Universität Karlsruhe, Germany, Heft 90, 1981, 127 pages.
- [25] H. Kishida, 'Behavior of a pile under horizontal cyclic loading', Proceedings of the International Conference on Soil Mechanics and Foundation Engineering, San Francisco, pp. 1413-1416.
- [26] C. Leblanc, G. T. Houlsby, and B. W. Byrne, "Response of stiff piles in sand to long-term cyclic lateral loading," *Geotechnique*, vol. 60, no. 2, pp. 79–90, 2010., doi:DOI: 10.1680/geot.7.00196.
- [27] C. Leblanc, B. W. Byrne, and G. T. Houlsby, "Response of stiff piles to random two-way lateral loading," *Geotechnique*, vol. 60, no. 9, pp. 715–721, 2010. DOI: 10.1680/geot.09.T.011
- [28] P. K. Peralta, Investigations on the Behavior of Large Diameter Piles under Long-Term Lateral Cyclic Loading in Cohesionless Soil, Degree of Doctor of Engineering. Hannover, Germany: Leibniz University, 2010.
- [29] Y. O. Barton and G. N. Pande, 'Laterally loaded piles in sand: centrifugal tests and finite elements analysis', Proceedings of the International Symposium on Numerical Models in Geomechanics, Zurich, September 13 to 17, 1982.
- [30] J. M. Ting, C. R. Kauffman, and M. Lovicsek, "Centrifuge static and dynamic lateral pile behaviour," *Can. Geotech. J.*, vol. 24, no. 2, pp. 198–207, 1987., doi:DOI: 10.1139/t87-025
- [31] L. Verdure, D. Levacher, and J. Garnier, (2003) 'Effet des cycles sur le comportement d'un pieu isolé dans un sable dense sous chargement latéral' (In French), *Revue Française de Géotechnique*, Vol. 7, No. 9, (2003), pp : 185-210. DOI: 10.1080/12795119.2003.9692541
- [32] P. Rosquoet, Pieux sous charge latérale cyclique (in French), Ph.D thesis, 2004, Ecole Centrale and University of Nantes, France.
- [33] J. Rakotonindriana, Comportement des pieux et des groupes de pieux sous chargement latéral cyclique (in French), Ph.D Thesis, 2009, Ecole Nationale des Ponts & Chaussées, France
- [34] Z. Li, S. K. Haigh, and M. Bolton, 'Centrifuge modelling of monopile under cyclic lateral loading', Proceedings of the Intl. Conf. on Physical Modelling in Geotechnics, ICPMG-2010, vol. 2. Zurich: Taylor and Francis Group, 2010, pp. 965–970.
- [35] A. Lyndon and R. Pearson, 'Skin friction effects on laterally loaded large diameter piles in sand', Proceedings of the conference Centrifuge'88, Paris 25-27 April, (1988), pp: 383-388.
- [36] E. Degny, SLIVALIC 5- Quintic spline smoothing program, LCPC, User's manual, Report ref. 1.05.10.4, 1985.
- [37] A. Bouafia, "Single piles under horizontal loads in sand: Determination of P–Y curves from the prebored pressuremeter test," *Geotech. Geol. Eng.*, vol. 25, no. 3, pp. 283–301, 2007., doi: 10.1007/s10706-006-9110-7.
- [38] A. Bouafia and J. Garnier, 'Behavior of a single pile loaded laterally in sand', Proceedings of the International Conference Deep Foundations, Paris. March 19-21, 1991.
- [39] J.-L. Briaud, *Geotechnical engineering: Unsaturated and saturated soils*, edited by John Wiley & Sons, Inc.
- [40] A. Bouafia, "Étude expérimentale du Chargement Latéral cyclique répété des pieux isolés dans le sable en Centrifugeuse," *Can. Geotech. J.*, vol. 31, no. 5, pp. 740–748, 1994., doi: 10.1139/t94-085.